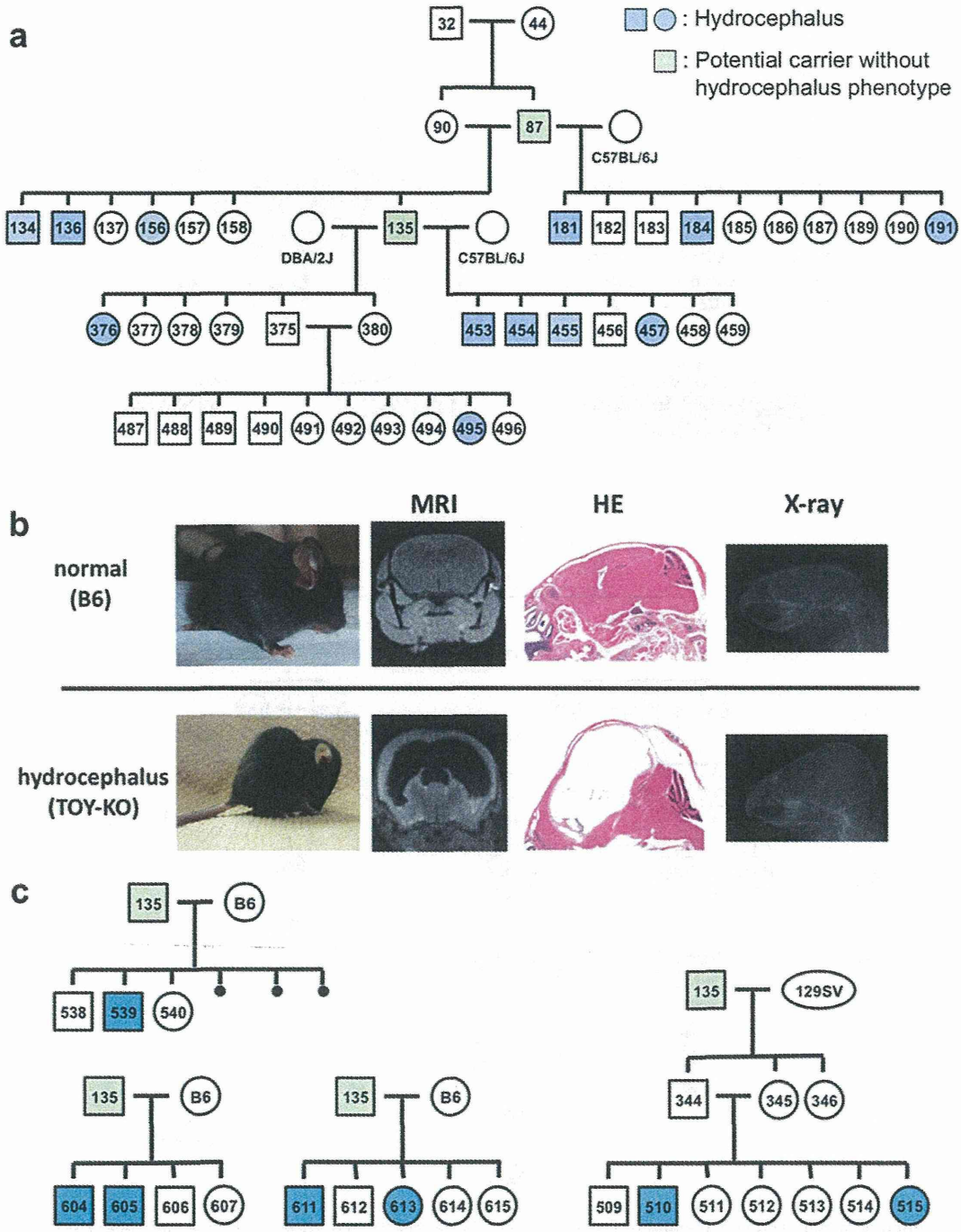

Figure 2 | Phenotypic variations observed in the progeny of TOY-KO mice. (a) The hydrocephalus trait was transmitted to the next generation in the TOY-KO pedigree. A hematoxylin/eosin-stained section showing the typical features of the hydrocephalus trait. Blue indicates a mouse with hydrocephalus, and green indicates a mouse carrying the causative mutation without the hydrocephalus phenotype (also shown in Supplementary Fig. S2 online). (b) Hydrocephalus. MRI, hematoxylin/eosin staining and X-ray images of normal (C57BL/6J) and hydrocephalus TOY-KO mice are shown in the upper panel. MRI images were obtained using an MRI mini SA (DS Pharma Biomedical Co. Ltd., Suita, Japan). X-ray images were obtained using a μFX-1000 (Fuji Photo File Co. Ltd.). (c) Pedigrees of the TOY-KO mouse mated with C57BL/6J (shown as B6) and 129Sv mice are shown in the lower panel. Blue indicates a mouse with hydrocephalus, and green indicates a mouse carrying the causative mutation without the hydrocephalus phenotype.

molecule for spontaneous G to T mutation in the mouse germ cell lineage. These mutations arose in all progeny of each generation and in all chromosomes that we analyzed (Figs. 4 and 5a). The mutations ranged from synonymous substitutions to harmful mutations, such as a gain of a stop codon in the *Ttn* gene responsible for human hypertrophic cardiomyopathy[18] (Supplementary Data S1 online).

By analyzing the position of the mutated G in di- and tri-nucleotide sequences, we found that G to T mutations occurred more often at GpC sites than at CpG sites, and tended to occur at tri-nucleotides, which are typical sequences found in triplet repeat expansion disorders (Fig. 5b, c), such as CAG (Huntington's disease), CTG (Myotonic dystrophy) and GAA (Friedreich ataxia)[19]. It is probable

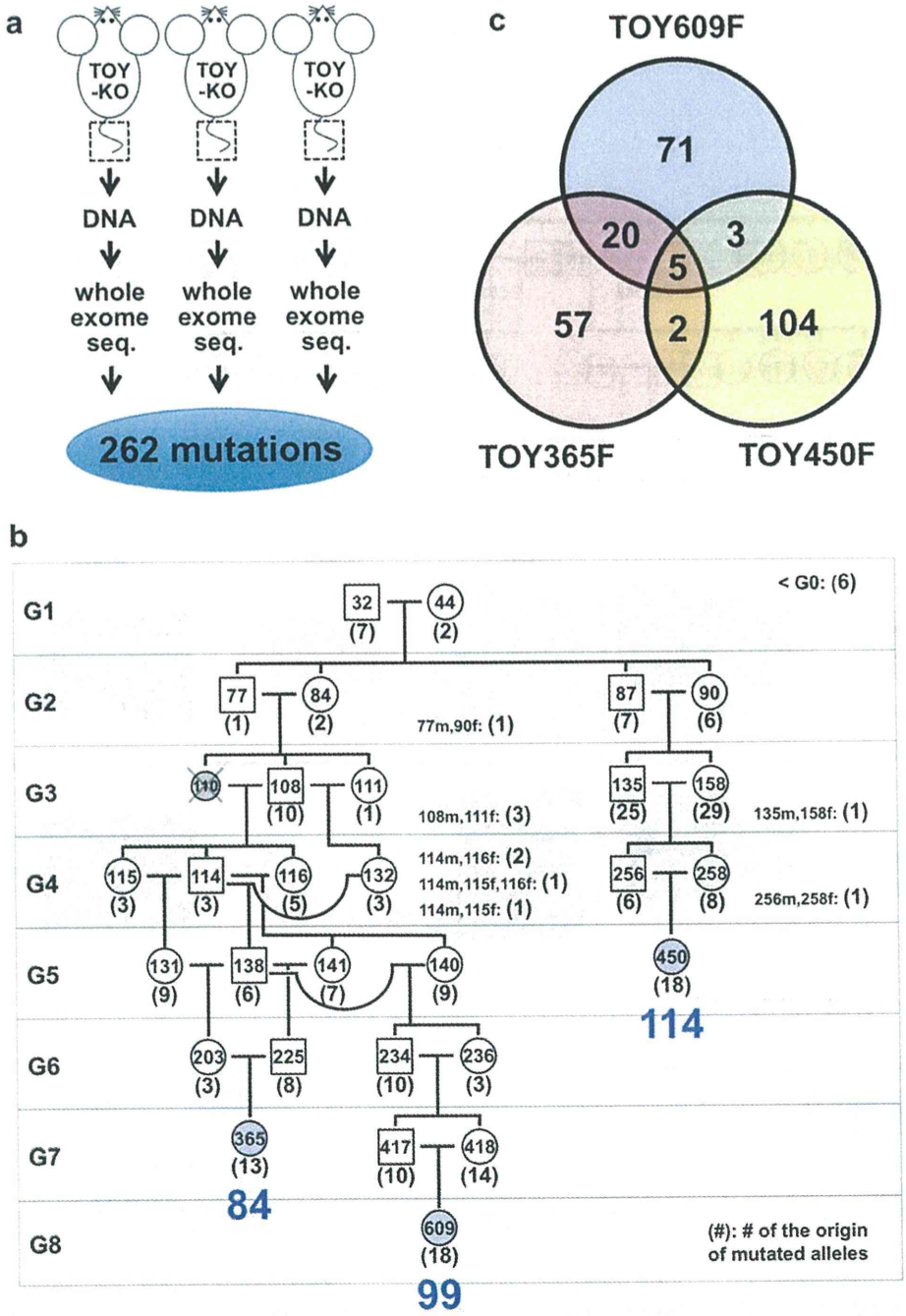

Figure 3 | Identification of *de novo* germline mutations in TOY-KO mice. (a) Scheme for screening of germline mutations. (b) Pedigree of TOY-KO mice used for germline mutation analysis. TOY365F, TOY609F and TOY450F were used to identify *de novo* germline mutations. Blue numbers, 84, 98, and 114, indicate the number of mutations detected in TOY365F, TOY609F and TOY450F, respectively. Numbers in parentheses indicate the number of original mutations in each generation, which were found in tail DNA for the first time in the pedigree. The DNA of TOY110F was unavailable; therefore, the mouse was excluded from the analysis. (c) The numbers of base substitution mutations found in TOY365F, TOY609F and TOY450F.

that uneven distribution of mutable 8-oxoG is reflected by the tendency for DNA oxidation, or by the site preference of DNA polymerases in incorporating 8-oxodGTP. We also detected two G to A and one A to G transition mutations that were classified as synonymous coding or intronic mutations (Table 1, Supplementary Data S1 online).

***De novo* germline mutation rate of TOY-KO mouse.** The detected mutations accumulated in TOY365F, TOY450F and TOY609F contained parts of the mutations that had occurred in the germ cells of the ancestral mice, because only half of the chromosomes derived from the father and mother had transmitted to the offspring via gametogenesis and fertilization in each generation. The numbers of newly arisen mutations detected only in TOY365F, TOY450F and TOY609F were 13, 18 and 18, respectively (Fig. 3b). Therefore, the *de novo* germline mutation rate was calculated to be 2.0×10^{-7}/base/generation ($13 + 18 + 18/3/40.9$ Mb $\times$ 2/generation). This mutation rate is 18-fold higher than the basal level, $1.1 \times$

Table 1 | Spectrum of heritable mutations in TOY-KO mice

	All	G2–G8
G:C to A:T	7	2
A:T to G:C	2	1
G:C to T:A	252	244
A:T to C:G	1	0
G:C to C:G	0	0
A:T to T:A	0	0
total	262	247

Mutations detected in the 40.9 Mb exome sequences of TOY365F, TOY450F, and TOY609F (Fig. 3a) were classified into mutation types. The mutations observed in G2–G8 mice (Fig. 3b) were considered as mutations that occurred in the TOY-KO germ cell lineage.

10^{-8} mutations/base/generation, calculated from the specific locus test in mice[20]. For human trio analysis[1], the germline mutation rate was calculated to be 1.2×10^{-8} mutation/base/generation, and the G to T transversion mutation was observed in about 9% of all mutations. These results indicated that an approximately 200-fold increase in G to T transversion mutations occurred in the TOY-KO mice. No G to A transition mutations occurred in TOY365F, TOY450F, and TOY609F (totaling 245.4 Mb); therefore, the background mutation level of the TOY-KO mouse was estimated to be less than 4.1×10^{-9} G to A transition mutation/base/generation. This background mutation level is not high compared with that in humans (4.9×10^{-9} G to A transition mutation/base/generation)[1].

Fates of *de novo* germline mutations. By following up the mutated alleles in the pedigree, we observed the fates of the *de novo* mutations, in which some were fixed and others were eliminated in later generations. As shown in Fig. 6, for example, mutation #187 initially appeared in TOY108M (G3) as a heterozygous allele, indicating that the mutation probably occurred in the germ cell lineage of the parents, either TOY77M or TOY84F, and was transmitted to the progeny. At G5, it became homozygous in TOY138M and TOY-131F, and thus fixed in the progeny. Conversely, in another branch, the mutant allele was not transmitted to the offspring and eventually disappeared. These behaviors of the mutated allele represent the appearance, transmission, fixation and disappearance of a spontaneous mutation, which are the typical fates of a novel mutation in the evolutionary process.

Discussion

Little research has been performed to identify the causative molecule of spontaneous germline mutations because it is a rare event. We considered that the causative molecule must possess certain features that make DNA more prone to mutation, be generated endogenously and spontaneously and remain in the germ cell lineage. In 2006, we reported that endogenous 8-oxoG is distributed in the genome of human lymphocytes in the steady state[5]. We hypothesized that 8-oxoG also exists in the genome of germ lineage cells, and is responsible for spontaneous *de novo* germline mutations, because 8-oxoG is endogenously generated by ROS derived from cellular respiration, and is known to cause transversion mutations. By disruption of the

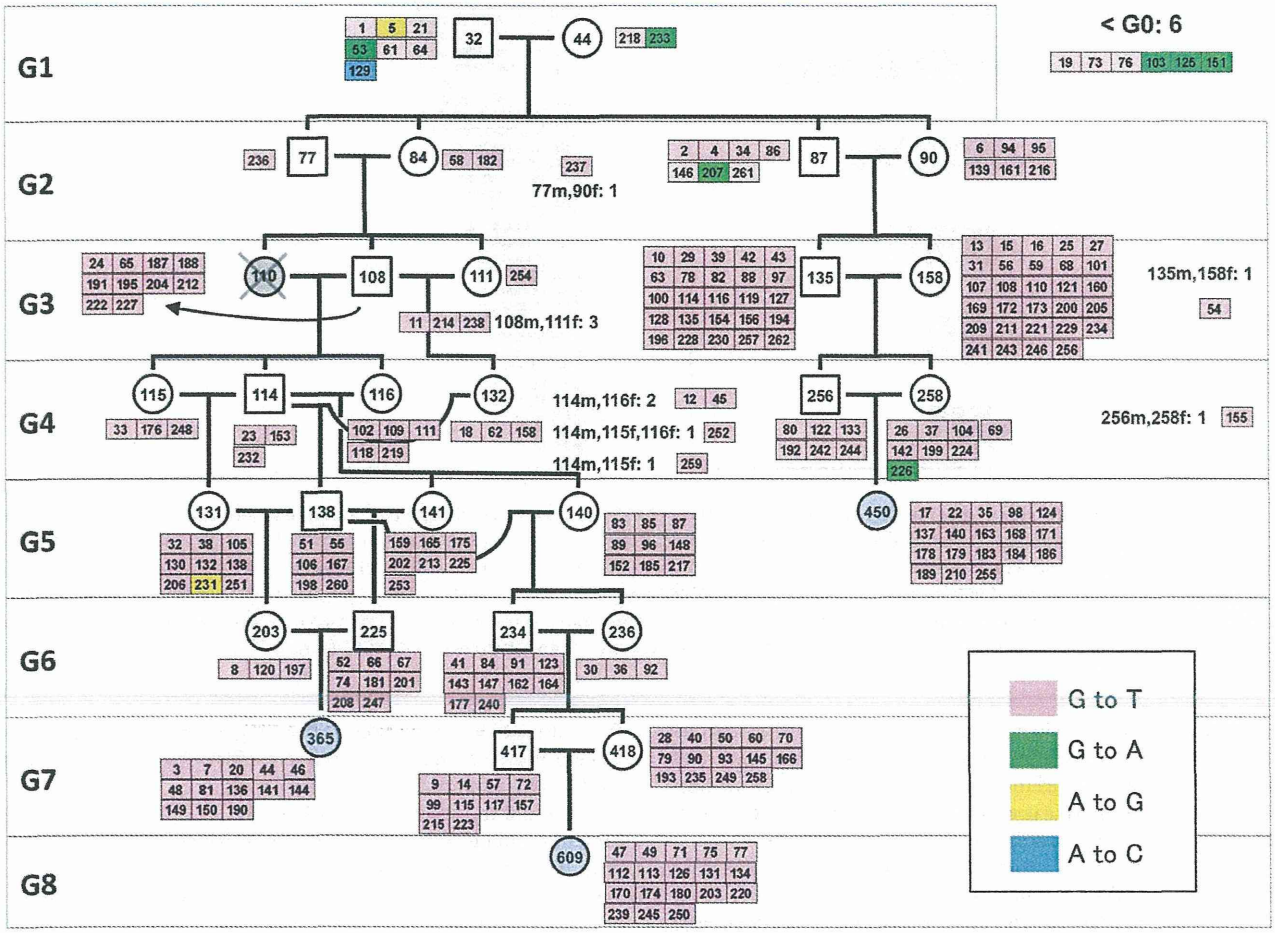

Figure 4 | Heritable mutations mapped in the pedigree of TOY-KO mice. The number in each box indicates the mutation ID number shown in Supplementary Data S1 online, and the color indicates the mutation category.

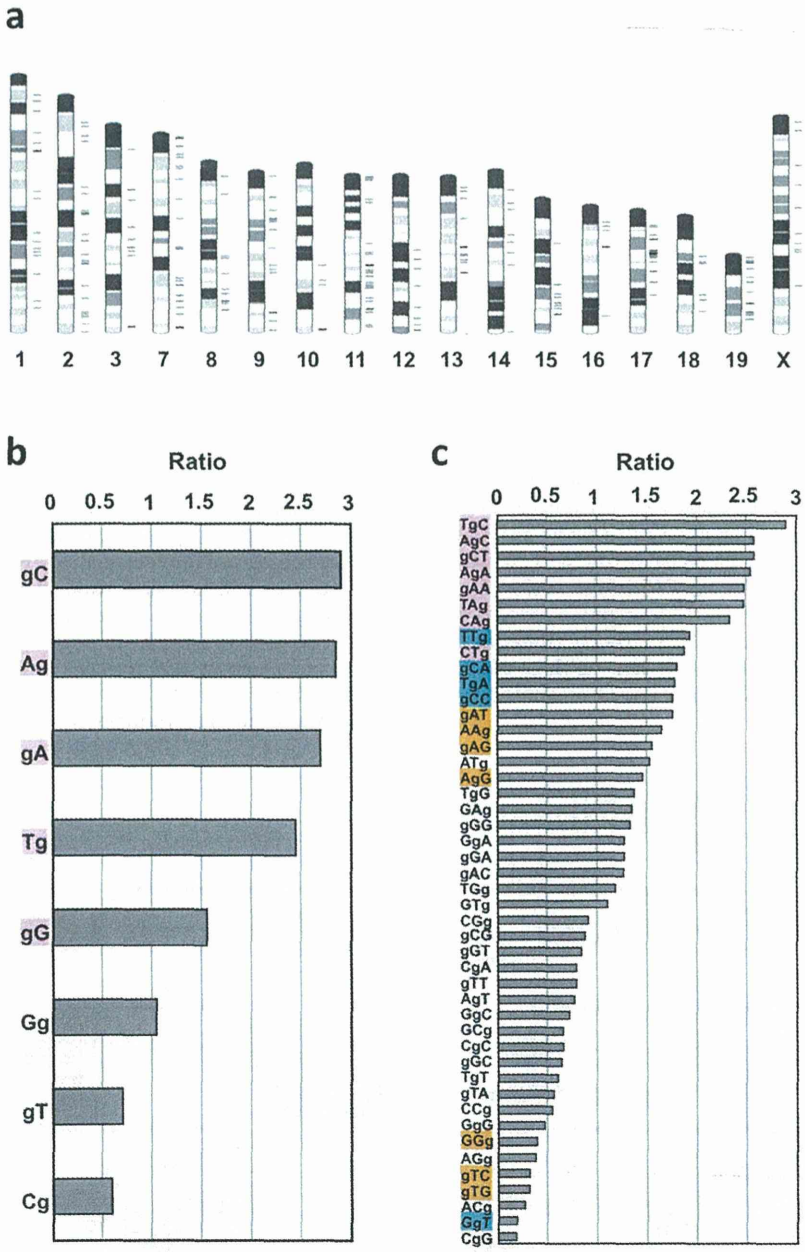

Figure 5 | Genome-wide distribution of mutations and site preferences of G to T mutations in di- and trinucleotide sequences. (a) Mutations detected in G2–G8 were mapped on a mouse G-band ideogram using Ideographica (http://www.ncrna.org/idiographica/). Each black transverse line on the right side of the chromosome represents a mutation site. (b) Site preferences of G to T mutations in di-nucleotide sequences. The plots represent the relative ratio of the actual value of detected mutations (G to T mutations in G2–G8) in each di-nucleotide to its occurrence level in the analyzed exome sequences. 'g' indicates the position of a mutated guanine. (c) Site preferences of G to T mutations in tri-nucleotides. For each nucleotide sequence, a chi square test (detected vs. expected) was performed, and the colored sequences indicate a significant difference: $P < 0.001$ (pink), $P < 0.01$ (blue), and $P < 0.05$ (orange).

8-oxoG exclusion system in mice, we detected increased spontaneous accumulation of germline mutations during the generations. These mutations were distributed throughout the chromosomes and inheritable to offspring across the generations, leading to an expansion of genetic diversity as well as disease-associated mutations.

The effects of 8-oxoG on spontaneous germline mutations were apparent in the TOY-KO mice. However, the production of 8-oxoG is dependent on the oxidation of guanine nucleotides, which occurs even in the wild-type cells independently of MTH1, OGG1 and MUTYH activities. It is likely that 8-oxoG universally causes *de novo* G-T transversion mutations, including germline mutations, although most of these mutations are efficiently prevented by the MTH1, OGG1 and MUTYH enzyme system.

When did the germline mutations occur? It is difficult to determine the timing of the occurrence of a mutation in the germ cell lineage; however, some examples were obtained that allowed us to speculate on the timing of mutations in our experiment. *De novo* mutations occur either in the germ cell lineage of the previous generation or during the very early developmental stage of the mutant mouse (Fig. 7). In eleven cases among 247 mutations, the mutations

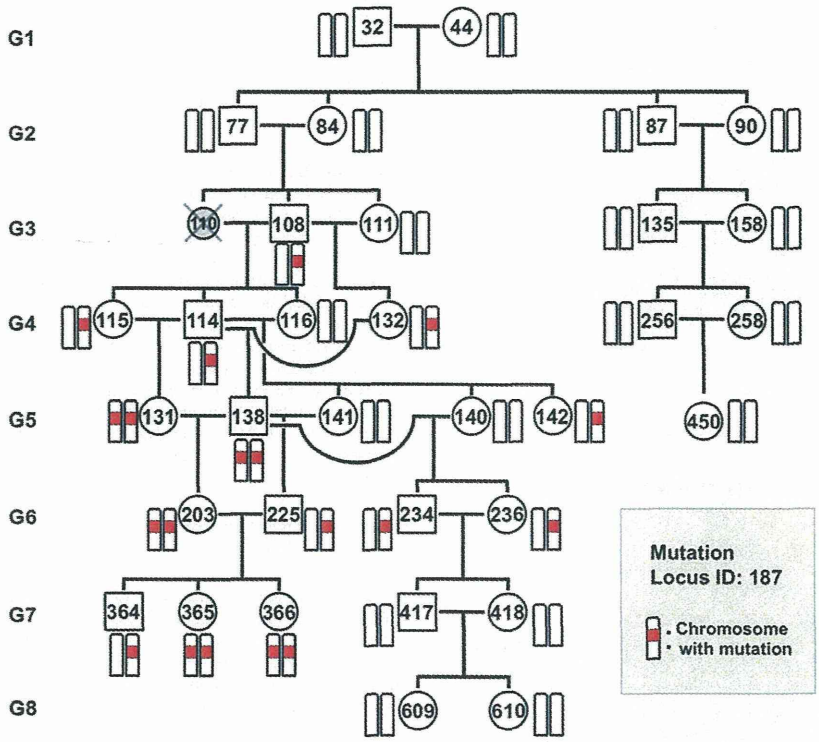

Figure 6 | Fate of a germline mutation. Mutation #187 (Ch. 15) was chosen to show the fate of a mutation generated in TOY-KO mice through the generations. This mutation initially appeared in TOY108M (G3) as a heterozygous allele. It was transmitted to progeny TOY-114M, TOY-115F, and TOY-132F. At G5, mutation #187 became homozygous in TOY138M and TOY131F, and thus were fixed in the progeny. Conversely, in another branch, the mutation was not transmitted from TOY-234M and TOY-236F (G6) to their offspring and eventually disappeared. The mutated locus is indicated in red.

had likely occurred in the germ cell lineage of the parents, because the original mutated allele was detected in multiple mice of the same generation (Fig. 3b). For three mutations on the X chromosome (Mutation ID #257, #261 and #262), which began in males with a heterozygous status (Supplementary Fig. S4 online), the mutation probably occurred in a cell at an early stage of embryonic development, resulting in mosaicism of tail tissue. These results showed that the germline mutations occurred at different developmental stages of the germ cell lineage. It is noteworthy that most germline mutations occurred during mitoses, because the germ cell lineage from fertilized egg to differentiated sperm or egg requires a large number of mitoses and only one meiosis. In the other cases (233/247) shown in Fig. 3b (G2–G8), the original mutated allele was found in a single mouse of each generation, and we could not identify when the mutation occurred.

By analogy to the *Escherichia coli* system, we considered that 8-oxoG-induced G to T mutation is suppressed by OGG1, MUTYH, and MTH1, whereas the A to C mutation is prevented by MTH1 in mammalian cells (Supplementary Fig. S5 online). However, in contrast to the *E. coli mutT, mutM, mutY* triple mutant, in which both G to T and A to C mutations increased[21], no A to C germline mutations were detected in the TOY-KO mouse. Thus, it is likely that different mechanisms, such as mismatch repair[22] or proof reading by DNA polymerase, may function to avoid A to C mutations caused by 8-oxodGTP in the TOY-KO mouse, even in the absence of MTH1. It has been reported that 2-hydroxy-deoxyadenosine (2-OHdA), an oxidized form of deoxyadenosine, is recognized as a substrate by the MUTYH protein and possesses premutagenic features[23,24]. 2-OHdATP, a triphosphate form of 2-OHdA, is a substrate of the MTH1 protein[25]. The MutY and MutT proteins of *E. coli* cannot recognize 2-OHdA, in contrast to the mammalian enzymes[24,26]. At the present, we cannot evaluate the contribution of 2-OHdA to the increase of germline mutation observed in TOY-KO mice, because we have not yet confirmed the accumulation of 2-OHdA in the DNA. Thus, the significance of 2-OHdA for germline mutations remains to be elucidated.

The TOY-KO mouse strain spontaneously accumulates mutations in the homozygous status. For genome-wide screening of mutants, this mouse has unique features and has the potential to take a complementary role to ENU mutagenesis[27,28]. The mutation is specific for G to T transversions, and occurs spontaneously and continuously in both male and female germ lineage cells of TOY-KO mice. The mutation rate of TOY-KO mice (0.2 mutation/Mb/generation, on average, in male and female) is lower than ENU-treated male gametes (1 mutation/0.42–1.82 Mb for male mouse[27], 1 mutation/3.7 Mb in male rat[28]); however, the number of mutations carried by each TOY-KO mouse increased as the generations increased. Similar to ENU mutagenesis, phenotype-driven screening is available. Currently, the TOY-KO mouse is only available in the C57BL/6J genetic background; however, it would be a good system for large genome-wide screening of dominant mutations. Using such mutator mice with a well-controlled genetic background would permit the evaluation of the contribution of aging and the difference between spermatogenesis and oogenesis on the accumulation of germline mutations. This system also enables us to assess the genotoxic effects of chemical and environmental factors on mammalian germ lineage cells.

Although *de novo* germline mutations cause sporadic genetic diseases in humans, their occurrence is an important step for the evolution of species, as well as selection for survival. 8-oxoG, one of the causative molecules of these mutations, is endogenously produced by ROS generated from biological processes, such as oxygen respiration

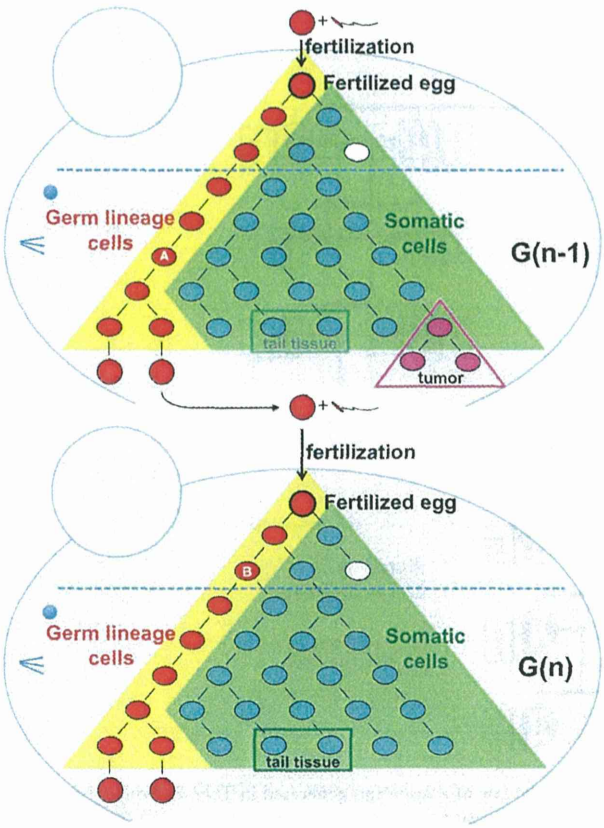

Figure 7 | Germ line mutations occur at different stages of the germ cell lineage. Mutations detected in the tail DNA of the first mutant mouse had occurred either in the germ lineage cells of the previous generation or during the very early developmental stage of the mutant mouse. Mutations start to accumulate from the first replication of fertilized egg DNA; however, each mutation is diluted out in the tissue DNA. Therefore, we used the tail DNA sequence as a reference sequence of fertilized egg DNA. In contrast to tail tissue, differentiated gametes can transmit their sequence information monoclonally to offspring. If the original mutated allele was mapped in multiple mice of the same generation, such as mutation #54 (in Fig. 4, Supplementary Data S1 online), the mutation probably occurred in the germ lineage cells of the parents (indicated as A). For mutations in the X chromosome (such as mutation #261), which began in the male with a heterozygous status (see Supplementary Fig. S4 online), the mutation probably occurred in a cell during the early stage of embryonic development (shown as B), resulting in mosaicism of tail tissue. These results indicate that germline mutations occur at different developmental stages of the germ cell lineage.

and inflammation, and is widely present in the DNA of various organisms. It is likely that the oxidative environment expands the genetic diversity of species by increasing the mutation rate of the germ lineage cells to accelerate the evolutionary process. MTH1, OGG1 and MUTYH, which are well conserved among species, may have contributed coordinately to control the germline mutation rate to an appropriate level for each species during evolution by controlling the amount of 8-oxoG in the genome (Supplementary Fig. S1 online).

Methods

Animals. *Mth1*$^{+/-}$, *Ogg1*$^{+/-}$, and *Mutyh*$^{+/-}$ mice were established[13,14,16] and backcrossed to C57BL/6J:Jcl (Clear Japan, Tokyo, Japan) for more than 16 generations. By crossing the C57BL/6J-background *Ogg1*$^{+/-}$, *Mth1*$^{+/-}$, and *Mutyh*$^{+/-}$ mice, we obtained *Mth1*$^{+/-}$/*Ogg1*$^{+/-}$ mice and *Ogg1*$^{+/-}$/*Mutyh*$^{+/-}$ mice. *Mth1*$^{+/-}$/*Ogg1*$^{+/-}$ mice were then mated with *Ogg1*$^{+/-}$/*Mutyh*$^{+/-}$ mice to obtain *Mth1*$^{+/-}$/*Ogg1*$^{-/-}$/*Mutyh*$^{+/-}$ mice. Finally, by crossing the *Mth1*$^{+/-}$/*Ogg1*$^{-/-}$/*Mutyh*$^{+/-}$ mice, we obtained a pair of *Mth1*$^{-/-}$/*Ogg1*$^{-/-}$/*Mutyh*$^{-/-}$ mice (TOY32M and TOY44F). All animals were maintained in a temperature-controlled (22 ± 2°C, 55 ± 5% humidity), specific pathogen-free room with a 12-h light-dark cycle. The care and use of all animals were performed in accordance with prescribed national guidelines, and the Animal Care and Use Committee of Kyushu University granted ethical approval for the study.

Quantification of 8-oxo-dG by LC-MS/MS. To detect the level of nuclear 8-oxodG, C57BL/6J:Jcl and TOY-KO mice (12–14 weeks old) were euthanized by cervical dislocation, and tissues were immediately removed and frozen in liquid nitrogen. DNA was extracted using a DNA Extractor TIS Kit (# 296-67701, Wako Pure Chemical Industries, Osaka, Japan), according to the manufacturer's instructions, with a slight modification: 10 mM 2, 2, 6, 6-tetramethylpiperidine-N-oxyl (Wako Pure Chemical Industries) was added to all reagents at all stages of manipulation[29]. Extracted DNA was hydrolyzed with 0.17 mg/ml nuclease P1 (Yamasa, Chiba, Japan) and 1.7 μM acid phosphatase (P-1435, Sigma-Aldrich Japan Inc., Tokyo, Japan) in 17 mM sodium acetate buffer (pH 4.5) at 37°C for 30 min, followed by filtration at 12,000 × *g* for 3 min (Ultrafree-MC probind 0.45 μm, Millipore, Billerica, MA). The digested samples (100 μl) were subjected to liquid chromatography-tandem mass spectrometry (LC-MS/MS) analysis using a Shimadzu VP-10 HPLC system connected to an API3000 MS/MS system (PE-SCIEX, SpectraLab Scientific Inc, Ontario, Canada).

Statistical analyses. Statistical analyses were conducted using JMP 9.02 (SAS Institute Japan, Tokyo, Japan).

Detection of germ line mutations by whole exome sequencing. Exome sequencing libraries for three TOY-KO mice (TOY365F, TOY450F and TOY609F) and five DBF1 (DBA/2J:Jcl × C57BL/6J:Jcl F1) mice as controls were prepared using a SureSelect^{XT} Mouse All Exon Kit (Agilent Technologies Japan, Tokyo, Japan), according to the manufacturer's instructions. Briefly, 3 μg of genomic tail DNA was sonicated into 150–180 bp fragments using a Covaris S2 System (Covaris, Woburn, MA, USA). The adaptors were ligated to the sonicated DNA after blunting and ~200 bp fragments were extracted using a 2% E-Gel (Life Technologies Japan, Tokyo, Japan). The extracted fragments were amplified with 2.5 mM SureSelect Pre-Capture primers and Platinum PCR Amplification Mix (Life Technologies), under the following conditions: 72°C for 20 min and 95°C for 5 min; 12 cycles of 95°C for 15 sec, 54°C for 45 sec and 70°C for 1 min; and a final extension at 70°C for 5 min. The PCR products were purified with a PureLink column (Life Technologies Japan). Purified PCR products (500 ng) were hybridized for 36 h at 65°C with SureSelect baits, according to the manufacturer's protocol. The captured libraries were amplified with the SureSelect Barcoding primer (BC1-8) for SOLiD with Herculase II Fusion DNA Polymerase (Agilent Technologies Japan), under the following conditions: 95°C for 5 min; 8 cycles of 95°C for 15 sec, 54°C for 45 sec and 70°C for 1 min; final extension at 70°C for 5 min. The captured barcoding libraries were quantified with an Agilent QPCR NHS Library Quantification Kit (Agilent Technologies Japan) and pooled. The four pooled libraries (1 pM) were amplified and purified with an EZ bead system (Life Technologies Japan). Purified P2-enriched beads were sequenced on one full slide of a SOLiD4 system (Life Technologies Japan). About 130 million paired-end sequencing reads (50 bp and 35 bp) were obtained from each library. Bioscope1.3.1 (Life Technologies Japan) was used to map the SOLiD paired-end reads to the mm9 reference mouse genome sequence (MGSCv37) using default parameters for Targeted resequencing methods. BEDtools v2.16.2 were used to calculate the coverage depth statistics and target enrichment efficiency. Avadis-NGS v1.3 (Strand Scientific Intelligence Inc., Karnataka, India) was used to carry out single nucleotide variant (SNV) calling with eight BAM format files (three TOY-KO lines and five control samples). The cutoff parameters of the SNV call were as follows: filtered sequencing quality ≤20, filtered PCR duplications, consensus base quality ≤50, total coverage <10, variants read depth <3, and the Decibel Score by Avadis-NGS v1.3 <50. The Decibel Score, read depth of the SNV allele and SNV allele frequency were used to sort these candidates. The iterative genomic viewer was used to check the candidates sequentially to eliminate apparent false positives. Finally, MassARRAY was used to select 286 mutation candidates for validation experiments (Supplementary Table S1 online).

Confirmation of mutations by sequencing. A MassARRAY3 Analyzer (Sequenom Inc, San Diego, CA) with iPLEX Gold Genotyping Reagent (Sequenom Inc) was used to validate the 286 candidates, according to the manufacturer's instructions. Briefly, MassARRAY Typer4 Assay Designer (Sequenom Inc) designed the 286 PCR primer pairs and 286 iPLEX primers as single-base extension primers for each candidate. We used 37 genomic DNA samples, including 35 samples from the TOY-KO pedigree and two control samples, as well as C57BL/6J and the original ES cell DNA to determine the origin of the *de novo* mutations in the TOY-KO pedigree. Ten nanograms of genomic DNA were used in each multiplex PCR for the MassARRAY. After dephosphorylation, single-base extension with the iPLEX primer and desalting were performed. The reaction products were spotted onto a 384-format SpectroCHIP with a MassARRAY Nanodispenser (Sequenom Inc) and then subjected to a MassARRAY 3 analyzer (Sequenom Inc). MassARRAY Typer 4.0 software (Sequenom Inc) was used to analyze the mass spectrum data.

Determination of the site preference of G to T mutation in di- and trinucleotide sequences. To analyze site preference of G to T mutation caused by *Mth1/Ogg1/Mutyh* deficiency, the 239 data of G to T mutation detected in G2–G8 were subjected (C to A mutations were converted to G to T mutation). The reference exon sequences and the 101 nucleotides those containing each mutation site (shown in Supplementary Data S1 online) were used to determine the site preference of mutation. The ratio shown in Fig. 5b, c were calculated as follows (data were summarized in Supplementary Table S2 online).

(A) The number of each di- or tri-nucleotides sequences in the reference exon sequence were counted by 1 nucleotide sliding.
(B) The number of each di- or tri-nucleotides sequences that include mutated guanine site were counted.
(C) The frequency of each di- or tri-nucleotides sequences was calculated as follows: (A) /number of total nucleotide in reference exon sequence.
(D) Total number of di- or tri-nucleotides sequences that include mutated guanine site were 478 and 717, respectively.
(E) The expected value for a random mutation for each di- or tri-nucleotides sequences were calculated as (C) × (D).
(F) The ratio (observed mutation for the expected value for a random mutation) was calculated as (B)/(E).

1. Kong, A. *et al.* Rate of de novo mutations and the importance of father's age to disease risk. *Nature* **488**, 471–475 (2012).
2. Keightley, P. D. Rates and Fitness Consequences of New Mutations in Humans. *Genetics* **190**, 295–304 (2012).
3. Xue, Y. *et al.* Deleterious- and disease-allele prevalence in healthy individuals: insights from current predictions, mutation databases, and population-scale resequencing. *Am. J. Hum. Genet.* **91**, 1022–1032 (2012).
4. Casals, F. & Bertranpetit, J. Human genetic variation, shared and private. *Science* **337**, 39–40 (2012).
5. Ohno, M. *et al.* A genome-wide distribution of 8-oxoguanine correlates with the preferred regions for recombination and single nucleotide polymorphism in the human genome. *Genome Res.* **16**, 567–575 (2006).
6. Shibutani, S., Takeshita, M. & Grollman, A. P. Insertion of specific bases during DNA synthesis past the oxidation-damaged base 8-oxodG. *Nature* **349**, 431–434 (1991).
7. Maki, H. & Sekiguchi, M. MutT protein specifically hydrolyses a potent mutagenic substrate for DNA synthesis. *Nature* **355**, 273–275 (1992).
8. Michaels, M. L., Cruz, C., Grollman, A. P. & Miller, J. H. Evidence that MutY and MutM combine to prevent mutations by an oxidatively damaged form of guanine in DNA. *Proc. Natl. Acad. Sci. U.S.A.* **89**, 7022–7025 (1992).
9. Sakumi, K. *et al.* Cloning and expression of cDNA for a human enzyme that hydrolyzes 8-oxo-dGTP, a mutagenic substrate for DNA synthesis. *J. Biol. Chem.* **268**, 23524–23530 (1992).
10. Radicella, J. P., Dherin, C., Desmaze, C., Fox, M. S. & Boiteux, S. Cloning and characterization of hOGG1, a human homolog of the *OGG1* gene of *Saccharomyces cerevisiae*. *Proc. Natl. Acad. Sci. U.S.A.* **94**, 8010–8015 (1997).
11. Rosenquist, T. A., Zharkov, D. O. & Grollman, A. P. Cloning and characterization of a mammalian 8-oxoguanine DNA glycosylase. *Proc. Natl. Acad. Sci. U.S.A.* **94**, 7429–7434 (1997).
12. McGoldrick, J. P., Yeh, Y. C., Solomon, M., Essigmann, J. M. & Lu, A. L. Characterization of a mammalian homolog of the *Escherichia coli* MutY mismatch repair protein. *Mol. Cell Biol.* **15**, 989–996 (1995).
13. Tsuzuki, T. *et al.* Spontaneous tumorigenesis in mice defective in the *MTH1* gene encoding 8-oxo-dGTPase. *Proc. Natl. Acad. Sci. U.S.A.* **98**, 11456–11461 (2001).
14. Sakumi, K. *et al. Ogg1* knockout-associated lung tumorigenesis and its suppression by *Mth1* gene disruption. *Cancer Res.* **63**, 902–905 (2003).
15. Xie, Y. *et al.* Deficiencies in mouse *Myh* and *Ogg1* result in tumor predisposition and G to T mutations in codon 12 of the *K-ras* oncogene in lung tumors. *Cancer Res.* **64**, 3096–3102 (2004).
16. Sakamoto, K. *et al.* MUTYH-null mice are susceptible to spontaneous and oxidative stress induced intestinal tumorigenesis. *Cancer Res.* **67**, 6599–6604 (2007).
17. Al-Tassan, N. *et al.* Inherited variants of MYH associated with somatic G:C T:A mutations in colorectal tumors. *Nat. Genet.* **30**, 227–232 (2002).
18. Satoh, M. *et al.* Structural analysis of the titin gene in hypertrophic cardiomyopathy: identification of a novel disease gene. *Biochem. Biophys. Res. Commun.* **262**, 411–417 (1999).
19. Orr, H. T. & Zoghbi, H. Y. Trinucleotide repeat disorders. *Annu. Rev. Neurosci.* **30**, 575–621 (2007).
20. Drake, J. W., Charlesworth, B., Charlesworth, D. & Crow, J. F. Rates of spontaneous mutation. *Genetics* **148**, 1667–1686 (1998).
21. Tajiri, T., Maki, H. & Sekiguchi, M. Functional cooperation of MutT, MutM and MutY proteins in preventing mutations caused by spontaneous oxidation of guanine nucleotide in *Escherichia coli*. *Mutat. Res.* **336**, 257–267 (1995).
22. Russo, M. T. *et al.* The oxidized deoxynucleoside triphosphate pool is a significant contributor to genetic instability in mismatch repair-deficient cells. *Mol. Cell Biol.* **24**, 465–474 (2004).
23. Kamiya, H. Mutagenicities of 8-hydroxyguanine and 2-hydroxyadenine produced by reactive oxygen species. *Biol. Pharm. Bull.* **27**, 475–479 (2004).
24. Ushijima, Y. *et al.* A functional analysis of the DNA glycosylase activity of mouse MUTYH protein excising 2-hydroxyadenine opposite guanine in DNA. *Nucleic Acids Res.* **33**, 672–682 (2005).
25. Fujikawa, K. *et al.* The oxidized forms of dATP are substrates for the human MutT homologue, the hMTH1 protein. *J. Biol. Chem.* **274**, 18201–18205 (1999).
26. Kamiya, H. & Kasai, H. 2-hydroxyadenine in DNA is a very poor substrate of the *Escherichia coli* MutY protein. *J. Radiat. Res.* **41**, 349–354 (2000).
27. Keays, D. A., Clark, T. G. & Flint, J. Estimating the number of coding mutations in genotypic- and phenotypic-driven *N*-ethyl-*N*-nitrosourea (ENU) screens. *Mammalian Genome* **17**, 230–238 (2006).
28. Mashimo, T. *et al.* An ENU-induced mutant archive for gene targeting in rats. *Nature Genetics* **40**, 514–515 (2008).
29. Tsuruya, K. *et al.* Accumulation of 8-oxoguanine in the cellular DNA and the alteration of the OGG1 expression during ischemia-reperfusion injury in the rat kidney. *DNA Repair* **2**, 211–229 (2003).

Acknowledgments

We thank N. Adachi for the LC-MS/MS analysis and A. Matsuyama, K. Nakabeppu, S. Kitamura, K. Asakawa, and T. Kuwano for technical support. This work was supported by grants from the Japan Society for the Promotion of Science (JSPS KAKENHI numbers: 20012038, 21240043, 21657002, 22300144, 22221004, and 25241016) and a Grant-in-Aid for JSPS Fellows (JSPS KAKENHI number 24·9979). This work was partly performed in the Cooperative Research Project Program of the Medical Institute of Bioregulation, Kyushu University.

Author contributions

M.O. and K.S. designed the study, analysed data, and wrote the paper. R.F. and Y.G. designed and performed exome and sequencing analyses. Y.I. and T.I. performed bioinformatic analysis. T.T. gave conceptual advice. M.F. quantitated 8-oxodG. M.H. analysed hydrocephalus mice. Y.N. was involved in the study design and preparation of the paper. All authors discussed the results and commented on the manuscript.

Additional information

Supplementary information accompanies this paper at http://www.nature.com/scientificreports

Competing financial interests: The authors declare no competing financial interests.

How to cite this article: Ohno, M. *et al.* 8-oxoguanine causes spontaneous *de novo* germline mutations in mice. *Sci. Rep.* 4, 4689; DOI:10.1038/srep04689 (2014).

IVYSPRING INTERNATIONAL PUBLISHER

International Journal of Biological Sciences

2014; 10(8): 940-947. doi: 10.7150/ijbs.9241

Research Paper

Abnormality in Wnt Signaling is Causatively Associated with Oxidative Stress-Induced Intestinal Tumorigenesis in MUTYH-Null Mice

Takuro Isoda[1, 2], Yoshimichi Nakatsu[1], Kazumi Yamauchi[1], Jingshu Piao[1], Takashi Yao[3], Hiroshi Honda[2], Yusaku Nakabeppu[4], and Teruhisa Tsuzuki[1] ✉

1. Department of Medical Biophysics and Radiation Biology, Faculty of Medical Sciences, Kyushu University, Fukuoka, Japan,
2. Department of Clinical Radiology, Graduate School of Medical Sciences, Kyushu University, Fukuoka, Japan,
3. Department of Human Pathology, School of Medicine, Juntendo University, Tokyo, Japan,
4. Division of Neurofunctional Genomics, Department of Immunobiology and Neuroscience, Medical Institute of Bioregulation, Kyushu University, Fukuoka, Japan,

✉ Corresponding author: Teruhisa Tsuzuki, Department of Medical Biophysics and Radiation Biology, Faculty of Medical Sciences, Kyushu University, Fukuoka 812-8582, Japan. Phone: +81-92-642-6141; fax: +81-92-642-6145; E-mail: tsuzuki@med.kyushu-u.ac.jp

Received: 2014.03.28; Accepted: 2014.08.04; Published: 2014.08.23

Abstract

MUTYH is a DNA glycosylase that excises adenine paired with 8-oxoguanine to prevent mutagenesis in mammals. Biallelic germline mutations of *MUTYH* have been found in patients predisposed to a recessive form of familial adenomatous polyposis (MAP: MUTYH-associated polyposis). We previously reported that *Mutyh*-deficient mice showed a high susceptibility to spontaneous and oxidative stress-induced intestinal adenoma/carcinoma. Here, we performed mutation analysis of the tumor-associated genes including *Apc*, *Ctnnb1*, *Kras* and *Trp53* in the intestinal tumors of *Mutyh*-deficient mice. In the 62 tumors, we identified 25 mutations in *Apc* of 18 tumors and 36 mutations in *Ctnnb1* of 36 tumors. Altogether, 54 out of the 62 tumors (87.1%) had a mutation in either *Apc* or *Ctnnb1*; no tumor displayed mutations simultaneously in the both genes. Similar to MAP, 60 out of 61 mutations (98.3%) were identified as G:C to T:A transversions of which 85% occurred at either AGAA or TGAA sequences. Immunohistochemical analyses revealed the accumulation of β-catenin in the nuclei of tumors. No mutation was found in either *Kras* or *Trp53* in the tumors. These results indicate that the uncontrolled activation of Wnt signaling pathway is causatively associated with oxidative stress-induced intestinal tumorigenesis in the *Mutyh*-deficient mice.

Key words: MAP, DNA repair, oxidative DNA damage, Wnt signaling pathway, mutagenesis

Introduction

Oxidative DNA damage appears to cause either mutagenesis or cell death, thereby resulting in various age-related diseases such as cancer and multi-organ dysfunction (1). 8-oxoguanine (8-oxoG), which is the major modified base found in the oxidized DNA, is highly mutagenic DNA lesion since DNA polymerases incorporate adenine as well as cytosine opposite 8-oxoG with almost equal frequency, thereby causing G:C to T:A transversion (2). In mammalian cells, 8-oxoG-related mutagenesis is prevented by MTH1, OGG1 and MUTYH. MTH1 has an 8-oxo-dGTPase activity hydrolyzing 8-oxo-dGTP to monophosphate form; 8-oxo-dGMP, thus preventing incorporation of 8-oxo-dGTP into DNA (3)(4), and found that MTH1 protein plays a crucial role in suppressing spontaneous mutagenesis as well as carcinogenesis (5)(6).

OGG1 is a DNA glycosylase that excises 8-oxoG paired with cytosine, and suppress spontaneous and UV-induced tumorigenesis in mammal (7)(8)(9)(10)(11)(12). MUTYH removes adenine misincorporated opposite 8-oxoG and also removes 2-hydroxyadenine (generated by oxidation of adenine) misincorporated opposite guanine (13)(14). We previously established *Mutyh*-deficient mice (15)(16), and showed that *Mutyh*-deficient mice had susceptibility to tumorigenesis, especially adenoma and adenocarcinoma in the intestinal tracts (17). We also showed that oral administration of $KBrO_3$, an oxidizing agent known to induce the 8-oxoG in the genome, dramatically enhanced the tumor-formations in small intestines of *Mutyh*-deficient mice (17).

MUTYH-associated polyposis (MAP) is a human hereditary colorectal polyposis caused by biallelic-inherited mutations in *MUTYH* (18)(19). The clinical features of MAP resemble to attenuated familial adenomatous polyposis (AFAP) characterized with less polyps and later onset than familial adenomatous polyposis (FAP) (20)(21)(22). A significant number of patients clinically diagnosed as adenomatous polyposis without germline mutations in *APC* are considered to carry *MUTYH* mutations. In most cases, polyps developed in MAP patients had mutations in *APC*, almost all of those were G:C to T:A transversions with the frequent occurrence in AGAA or TGAA sequence (18)(23)(24).

APC is an important factor of the canonical Wnt-signaling pathway, and *APC* mutations cause a failure in phosphorylation of β-catenin by glycogen synthase kinase 3 beta (GSK3β), resulting in the stabilization of β-catenin and its accumulation in nucleus without Wnt signal. High level of β-catenin in nucleus leads to up-regulation of various genes for such as c-Myc and Cyclin D1 with T-cell factor/lymphoid enhancing factor (TCF/LEF) (25)(26). *APC* is also known as the tumor suppressor gene, germline mutation of which is responsible for FAP (27)(28). Somatic *APC* mutations were found in more than 80% of sporadic colorectal cancers (CRCs) and *CTNNB1* (β-catenin) mutations were also found in about a half of CRCs lacking *APC* mutation (25)(29)(30). Because *APC* and *CTNNB1* mutations are mutually exclusive, it is considered that each mutation has nearly equal effect on β-catenin stability and TCF/LEF transactivation, albeit some differences such as the effect on invasiveness (31). Accordingly, unrestrained activation of the Wnt signaling pathway, resulted from the mutations in *APC* or in *CTNNB1*, is considered to be associated with early premalignant lesion, such as aberrant crypt foci and small polyps (32).

In addition to *APC* or *CTNNB1*, mutations in *KRAS* and *TP53* are frequently found in colorectal cancer in human. *KRAS* mutations, mainly at codon 12, were found in approximately a half of colorectal cancers (26)(33)(34). *TP53* (official symbol: *TP53* in human, and *Trp53* in mouse) is a tumor suppressor gene involved in various cellular functions, such as cell-cycle control, apoptosis and maintenance of genetic stability. Defects of *TP53*, resulting from mutations or loss of heterozygosity, were found in many of colorectal cancers (35)(36). *KRAS* mutations, but not *TP53* mutations, are commonly observed in tumors from MAP patients (37)(38).

In this study, we performed pathological evaluation among the small intestinal tumors developed in wild-type and *Mutyh*-deficient mice treated with $KBrO_3$ according to the Vienna classification of gastrointestinal epithelial neoplasia (39). To gain an insight into the process of the oxidative stress-induced tumor-development in *MUTYH*-deficient genetic background, we analyzed mutations in the tumor-associated genes, such as *Apc*, *Ctnnb1*, *Kras* and *Trp53* in the tumors developed in wild-type and *Mutyh*-deficient mice treated with $KBrO_3$.

Materials and methods

Animals and $KBrO_3$ treatment

Mutyh-deficient mice used in this study were previously generated, and backcrossed to C57BL/6J for more than 10 generations (17). Genomic DNA samples and histological slides of the small intestinal tumors were prepared from the mice treated with $KBrO_3$ as previously reported (17). Briefly, wild-type C57BL/6J mice or congenic *Mutyh*-deficient mice were treated with 0.2% $KBrO_3$ in drinking water for 16 weeks. Body weight and amount of water consumption were measured once a week. At the end of the $KBrO_3$-treatment, mice were sacrificed and the tissues were fixed with 4% buffered-formaldehyde and then stored in 70% ethanol. All animals were kept in specific pathogen free (SPF) conditions. All animal care and handling procedures were approved by the Institutional Animal Care and Use Committee of Kyushu University, and followed the Guideline for Proper Conduct of Animal Experiments, Science Council of Japan.

Preparation of DNA from small intestinal tumor

Inspections of the small intestines were carefully carried out and the small intestinal tumors were removed under dissecting microscope. Preparations of DNA from the removed tumors were performed using DNeasy Tissue Kit (QIAGEN) according to the manufacturer's protocol.

PCR and DNA sequencing

Sixty-two small intestinal tumors obtained from 4 *Mutyh*-deficient mice were used for mutation analysis of *Apc, Ctnnb1, Kras* and *Trp53*, while 11 tumors developed in wild-type mice were analyzed for mutations only in *Ctnnb1*. Thirty- to fifty-nanogram of genomic DNA from each small intestinal tumor was used as the template for PCR. Amplified DNA was purified with QIAquick PCR Purification Kit (QIAGEN) according to the manufacturer's protocol. The purified DNA fragments were used as the template for direct sequencing with BigDye Terminator v3.1 Cycle Sequencing kit (Applied Biosystems) and the sequences were determined with ABI PRISM® 3100 Genetic Analyzer (Applied Biosystems). In the case of detecting two mutations in *Apc* from one tumor, we performed PCR with new primer sets designed for amplifying the fragment encompassing both mutation sites. The DNA fragments amplified with PrimeSTAR HS DNA polymerase (TAKARA) were inserted into the EcoRV site in pBluescript II SK(-) (Stratagene) and the cloned fragments were used as templates for sequencing. In the case of deletion found by direct sequencing, we confirmed the deleted region by sequencing using cloned amplified fragment as template. The information of the primers used and PCR conditions are available upon request.

Histological analysis

The small intestinal tumors were removed, embedded in paraffin and sectioned (3 μm). After being deparaffinized and re-hydrated, the sections were stained with hematoxylene and eosin. The evaluation of the tumors was performed according to the Vienna classification (39).

Immunohistochemistry

Immunohistochemistry were performed on 3 μm thick paraffin-embedded sections of the small intestinal tumors with anti-β-catenin antibody. The sections were deparaffinized in xylen and re-hydrated through graduated ethanol at room temperature. Tissue sections were soaked in 10 mM citrate buffer (pH6.0) and then subjected to antigen retrieval by microwaving for 20 minutes before the primary antibodey reaction. After treatment with 3% hydrogen peroxide for 5 minutes and 50 mM Tris-HCl (pH7.5) containing 1% BSA for 15 minutes, a 1:4000 diluted rabbit polyclonal anti-β-catenin antibody (Sigma) was applied to the sections, and incubated either at room temperature for 1 hr or at 4°C overnight. The detections were carried out with avidin-biotin-enzyme complex (ABC) method using LSAB+ System-HRP (DAKO) according to the manufacturer's protocol. The tumors with more than 5% of nuclear stained cells were counted for positive.

Results

Pathological analysis of small intestinal tumors

We performed pathological analysis of 73 and 10 small intestinal tumors derived from *Mutyh*-deficient (n=4) and wild-type mice (n=10), respectively (Table 1, Figure 1). The tumors had predominantly developed in the oral side of the small intestine. The sizes of the tumors developed in wild-type mice were apparently smaller than those in *Mutyh*-deficient mice. All tumors showed non-polypoid growth and their height was almost equal to normal villi. All the tumors showed cytological changes such as variably sized and enlarged nuclei, and also showed architectural changes with keeping the fundamental structure of glands, while no tumors showed evident invasion. Based on the Vienna classification of gastrointestinal epithelial neoplasia, all of these tumors were classified as category 4 (non-invasive high grade neoplasia), except for one case in a wild-type mouse that was classified as category 3 (non-invasive low grade neoplasia) because of milder cytological and architectural changes.

Table 1. Pathological evaluation of $KBrO_3$-induced small intestinal tumors

	Category 3	Category 4			Total
		4.1	4.2	4.3	
Wild type mice	1	3	6	0	10
Mutyh-deficient mice	0	2	71	0	73

NOTE: The numbers in the table indicates the number of the tumors classified as each category. This evaluation was performed according to the Vienna classification of gastrointestinal neoplasia. Category 3: non-invasive low grade neoplasia, Category 4: non-invasive high grade neoplasia (4.1: high grade adenoma/displasia, 4.2: non-invasive carcinoma, 4.3: Suspicion of invasive carcinoma).

Somatic *Apc* mutations in the small intestinal tumors

To analyze *Apc* mutation, we amplified and sequenced the 5'-region of exon 15 of *Apc*, because many somatic mutations in this region were identified in the tumors from MAP patients (18)(23). Using 10 overlapping primer sets, the targeting region of *Apc* was amplified and used as templates for direct sequencings. We analyzed 62 tumors developed in 4 *Mutyh*-deficient mice treated with $KBrO_3$. Twenty-five somatic mutations from 18 tumors were detected, and all the mutations were identified as G:C to T:A transversions, leading to the non-sense mutations (Table 2). Seventeen out of 25 mutations (68.0%) were found in the AGAA or TGAA sequences. Because 7 tumors displayed two mutations in the region analyzed, we